

## Accelerator Version of the Intensive Lithium Antineutrino Source

V.I. Lyashuk <sup>§</sup>

*Institute for Nuclear Research of the Russian Academy of Sciences, Moscow, Russia*

The combination of decay parameters of the neutron-rich  $\beta^-$ -decaying  $^8\text{Li}$  isotope (short  $T_{1/2} = 0.84$  s) and its hard spectrum ( $E_{\bar{\nu}}^{\text{max}} = 13$  MeV and  $\langle E_{\bar{\nu}} \rangle = 6.5$  MeV) of well-known distribution allow to consider  $^8\text{Li}$  as a very perspective candidate for the artificial antineutrino source. The source can be produced at  $(n,\gamma)$ -activation of the starting  $^7\text{Li}$  isotope. Creation of the  $^8\text{Li}$  source can be realized in the tandem scheme of the proton accelerator with neutron producing heavy metal target inside the lithium blanket. The accelerator variant is optimized in efficiency of  $^8\text{Li}$  generation and in dimension that is exclusively important for investigation of oscillation in problem of sterile neutrino search in case of  $\Delta m^2 \sim 1 \text{ eV}^2$  scale. The analysis of  $^8\text{Li}$  creation in the lithium blanket-converter allowed to decrease its outer size down to  $\sim 70$  cm strongly decreasing the escape of neutrons from the source construction.

### 1. Introduction. Advantage of the Lithium Antineutrino Spectrum Compare to Reactor Spectrum

Starting from the pioneer works of F. Reines and C. L. Cowan in 1953 up today the reactors continue to be the uneclipsed steady source of electron antineutrino for scientists as for flux as for cost of experiments [1]. But in spite of the apparent superiority on neutrino flux the nuclear reactors has a disadvantage: too-small hardness of  $\bar{\nu}_e$ -spectrum, which rapidly decreases and lies below 10 MeV [2]. The next serious problem of the reactor spectrum is the large errors. So, the authors of the work [3] concluded that the reactor  $\bar{\nu}_e$ -spectrum is known with averaged accuracy of less than  $\sim 4\%$  and the level of accuracy can be caused by data on  $\sim(25-30)\%$  of forbidden transfers at decay of the main fuel isotopes ( $^{235}\text{U}$ ,  $^{239}\text{Pu}$ ,  $^{238}\text{U}$ ,  $^{241}\text{Pu}$ ). The composition strongly varies in time in operation period [4] and in case of reactor stops. The changing in composition leads to variation in  $\bar{\nu}_e$ -fluxes which are recalculated by means of correction factors for fuel isotopes. An additional unaccounted errors for  $\bar{\nu}_e$ -flux evaluation appear during reactor stops due to permanent presence of cooling pond for spent fuel. These errors can rise up to 1% compare to the operating reactor spectrum. It is usually considered that partial neutrino spectra  $N_{\bar{\nu}}^i$  (where  $i$  is the fuel isotope) reach equilibrium conditions after 1 day from the reactor life time. But this evaluation must be corrected too as the summary spectrum increases from the beginning to the end of the reactor life time on the value  $(5-6)\%$  in the region  $(1.8-3.0)$  MeV. [5]. The experimental detection of the bump in the reactor  $\bar{\nu}_e$ -spectrum added one more puzzle in interpretation of reactor  $\bar{\nu}_e$ -experiments [6].

For the purpose of the artificial neutrino source the  $^8\text{Li}$  isotope is characterized by undoubted advantage in  $\bar{\nu}_e$ -spectrum over the reactor one. The  $\bar{\nu}_e$ -spectrum of neutron-rich  $^8\text{Li}$  ( $\beta^-$ -decay with  $T_{1/2}=0.84$  s) is hard and well investigated: the maximal energy reaches  $\sim 13$  MeV with average value 6.5 MeV [7], that exclusively important for detection rate owing

---

<sup>§</sup> lyashuk@itep.ru

to the squared proportionality of the cross section to the neutrino energy  $\sigma_\nu \sim E_\nu^2$  for the considered “reactor” energy range.

The natural lithium consists of  ${}^7\text{Li}$  and  ${}^6\text{Li}$  – two stable isotopes with 92.48% and 7.52% weight parts correspondingly. For creation of the intensive  ${}^8\text{Li}$  electron antineutrino source at  ${}^7\text{Li}(n,\gamma){}^8\text{Li}$ -activation we need to exclude maximally the negative factor of strong neutron absorption at  ${}^6\text{Li}(n,\alpha)\text{T}$  process. The both cross sections follows to  $1/v$  law ( $v$  is velocity) at  $E_n \leq 1$  keV and at the thermal point  $E_n = 0.0253$  eV the cross section relation  $\sigma_{n,\alpha}({}^6\text{Li})/\sigma_{n,\gamma}({}^7\text{Li})$  is equal to (940 b / 0.045 b) according to TENDL-2019 and CENDL-3.2 neutron data libraries [8,9]. Clearly, that realization of the task is possible at high grade of  ${}^6\text{Li}$  removal: the proposed (and considered in this work) purification on  ${}^7\text{Li}$  is 99.99% [10, 11].

## 2. Antineutrino Source for the Scheme with Proton Accelerator. Compact Variant of the Source

Since the 70-th years of the XX-th century the possibility to apply the accelerator driven system on the base of spallation reaction for creation of the powerful neutron source began attract more and more attention and were realized and are constructing (ISIS, IN-06, JSNS/J-Park, KENS, LANSCE, SINQ, SNS, CSNS, ESS et al.). The large benefits of spallation neutron source (with targets usually made from tungsten, lead, tantalum, bismuth, uranium, mercury) is caused by the fact that as the proton energy is increasing the neutron yield  $Y_n$  (per proton) is increasing sharply: so, for heavy targets and proton energy  $E_p = 200\text{--}300$  MeV the neutron yield is about  $Y_n \approx (1.6\text{--}3.5)$ , for  $E_p = 500\text{--}600$  MeV the yield increases up to  $Y_n \approx 10$ .

In accelerator driven systems for creation of intensive neutrino source by  ${}^7\text{Li}(n,\gamma){}^8\text{Li}$  activation we proposed to surround the target by lithium blanket-converter [12]. It was investigated the neutron yield and creation of  ${}^8\text{Li}$  in the scheme of lithium blanket around the target (bombarded by proton of energy 50–300 MeV) manufactured from the lead, bismuth and tungsten (see Fig.1–2). The last has the high resistance to radiation damage under intensive proton beams and was considered as the main candidate for the target [13,14].

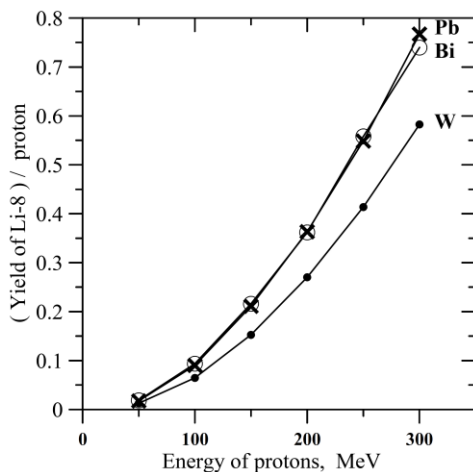
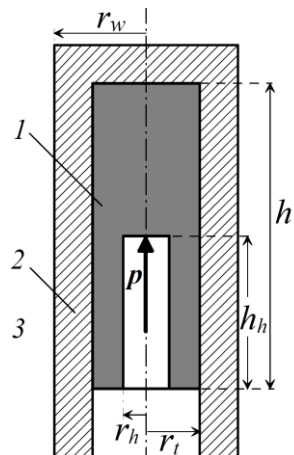


Fig. 1. Yield of  ${}^8\text{Li}$  for lead, bismuth and tungsten target depending on the proton energy.



Dimension of the compact neutrino source (in Fig. 3–4):

$$r_w = 12 \text{ cm,}$$

$$r_t = 7 \text{ cm,}$$

$$r_h = 3 \text{ cm,}$$

$$h_t = 30 \text{ cm,}$$

$$h_h = 20 \text{ cm;}$$

$p$  – proton beam.

Fig. 2. Geometry of the tungsten neutron producing target. 1 – tungsten target; 2 –  $\text{D}_2\text{O}$ -cooler; 3 – lithium blanket-converter.

Such not high energies are considered with purpose to decrease the possible background in neutrino experiments and intensive  $\pi^0$ -meson production (generating the electron-photon showers) which occurs at higher energies. From the beginning of the accelerator variant of the  $\bar{\nu}_e$ -source investigation the blanket is considered in the cylindrical geometry (3.4 m in length, radial thickness – 1.7 m and central  $^{174}\text{W}$ -target cooled by heavy water). For the blanket substance we used the heavy water solution of  $^7\text{LiOD}$  with concentration 9.5% and 99.99% purification of  $^7\text{Li}$  [13,14].

For the constructed now JUNO neutrino detector [15] it was demonstrated that the lithium blanket can be perspective  $\bar{\nu}_e$ -source for search of sterile neutrinos. The obtained results reveals that sensitivity to the mixing-angle may be extremely high:  $\sin^2(2\theta) \leq 0.001$  for  $\Delta m^2 \gtrsim 0.2 \text{ eV}^2$  in the model (3+1) of three active plus one sterile neutrino [16].

The simulation of the possible sterile neutrino oscillation requested to take into account the distribution of  $^8\text{Li}$  yield in the blanket (i. e., distribution of the  $\bar{\nu}_e$ -source) [17–19]. For this purpose the blanket was divided into cells: 10 equal steps in length and 10 equal layers in radius. The summary number of created cells was 105 ones including five nonstandard cells after the target. The obtained  $^8\text{Li}$  yield in the cells confirmed the think to diminish the size of the neutrino source by separating of the central volume with more high yield (which ensure 68% of the total  $^8\text{Li}$  yield in the volume with dimension – 136 cm in length and 97 cm in radius) from outer space (which would be source shield with function of neutron moderator and reflector). In order to prevent the neutron escape from the diminished size of lithium blanket the (above mentioned) outer space was filled by carbon and water ( $\text{D}_2\text{O}$  or  $\text{H}_2\text{O}$ ).

The next steps in developing of more compact source for verification of the sterile neutrino models in short base line experiments (considering the cases of  $\Delta m^2 \sim \text{eV}^2$ ) [20–24]) are also dictated by possible errors caused by source dimension. In order to diminish the source size we base on the principle idea to increase strongly the rate of  $^7\text{Li}(n,\gamma)^8\text{Li}$  reaction close to the target. Simultaneously it is need to ensure an effective neutron moderation near the target too. We propose an effective solution – to insert the thin  $^7\text{Li}$  metal layer close to the tungsten target. Indeed, the nuclear concentration of  $^7\text{Li}$  nuclei in the lithium metal (with purification 99.99% on  $^7\text{Li}$ ) is higher than it concentration in the outer heavy water solution of  $^7\text{LiOD}$  in ~18 times. In analysis of the  $^8\text{Li}$  yield distribution the source volume was divided into small cells similar to the works [17,18]. The layer shield of the source was optimized to decrease the neutron flux from the installation that allowed to strongly decrease the escape of neutrons down to ~0.2% per proton. The scheme of the proposed  $\bar{\nu}_e$ -source and it dimension is presented in the Fig.3a and Fig.3b.

The idea to insert the thin  $^7\text{Li}$  layer for diminishing the size (and at the same time to ensure the high of  $^8\text{Li}$  yield) was confirmed in the simulation at the proton energy  $E_p = 200 \text{ MeV}$ . At the source length  $L = 70 \text{ cm}$  the obtained  $^8\text{Li}$  yield is  $k_p = 0.113$  compare to: 1)  $k_p = 0.072$  for the blanket with homogeneous heavy water  $\text{LiOD}$ -solution (i.e., without the lithium metal layer) and 2)  $k_p = 0.175$  in the previous case [18,19] with  $L = 136 \text{ cm}$ . But 68% of created  $^8\text{Li}$  nuclei are generated in the thin  $^7\text{Li}$  metal layer, i.e., within the volume at the radius  $R = (22–27) \text{ cm}$ . The Fig. 4 illustrates yield  $Y_{^8\text{Li}}$  of  $^8\text{Li}$  in the blanket cells and strong increase of the yield in the thin  $^7\text{Li}$  metal layer compare the case of heavy water  $\text{LiOD}$  solution. The total mass of the  $^7\text{Li}$  in the diminished lithium blanket (including  $\text{LiOD}$  solution plus metal layer) is 67.5 kg compare to 128.3 kg of the previous geometry [17–19].

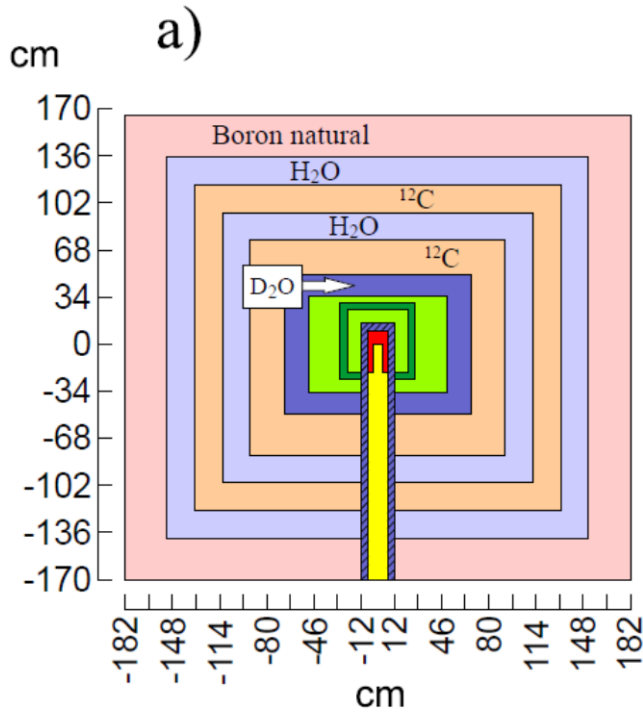


Fig.3a. Geometry of the lithium  $\bar{\nu}_e$ -source in the accelerator driven system. The all dimensions are given on the axes. Materials of zones around the central lithium volume with tungsten target (see Fig.3b) and channel of the proton accelerator are indicated.

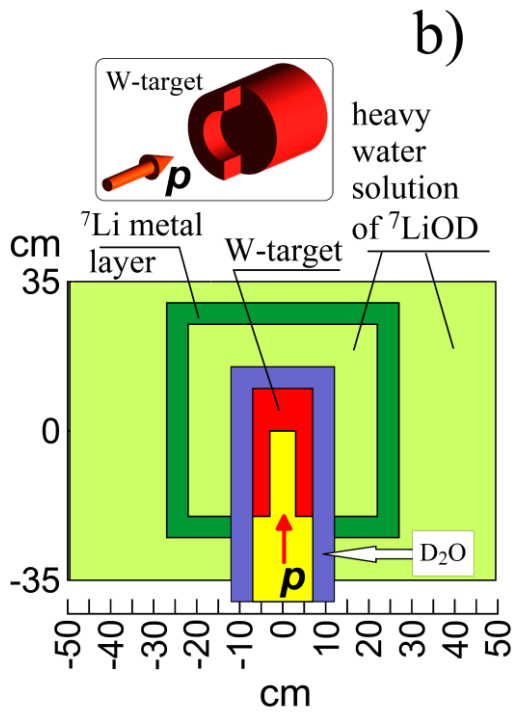


Fig. 3b. The magnified scheme of the central part of the lithium-  $\bar{\nu}_e$ -source (the tungsten target and lithium zones:  ${}^7\text{LiOD}$ -solution,  ${}^7\text{Li}$ -metal layer,  ${}^7\text{LiOD}$ -solution). The all dimensions of zones around the central lithium volume with tungsten target and channel of the proton accelerator are given on the axes.

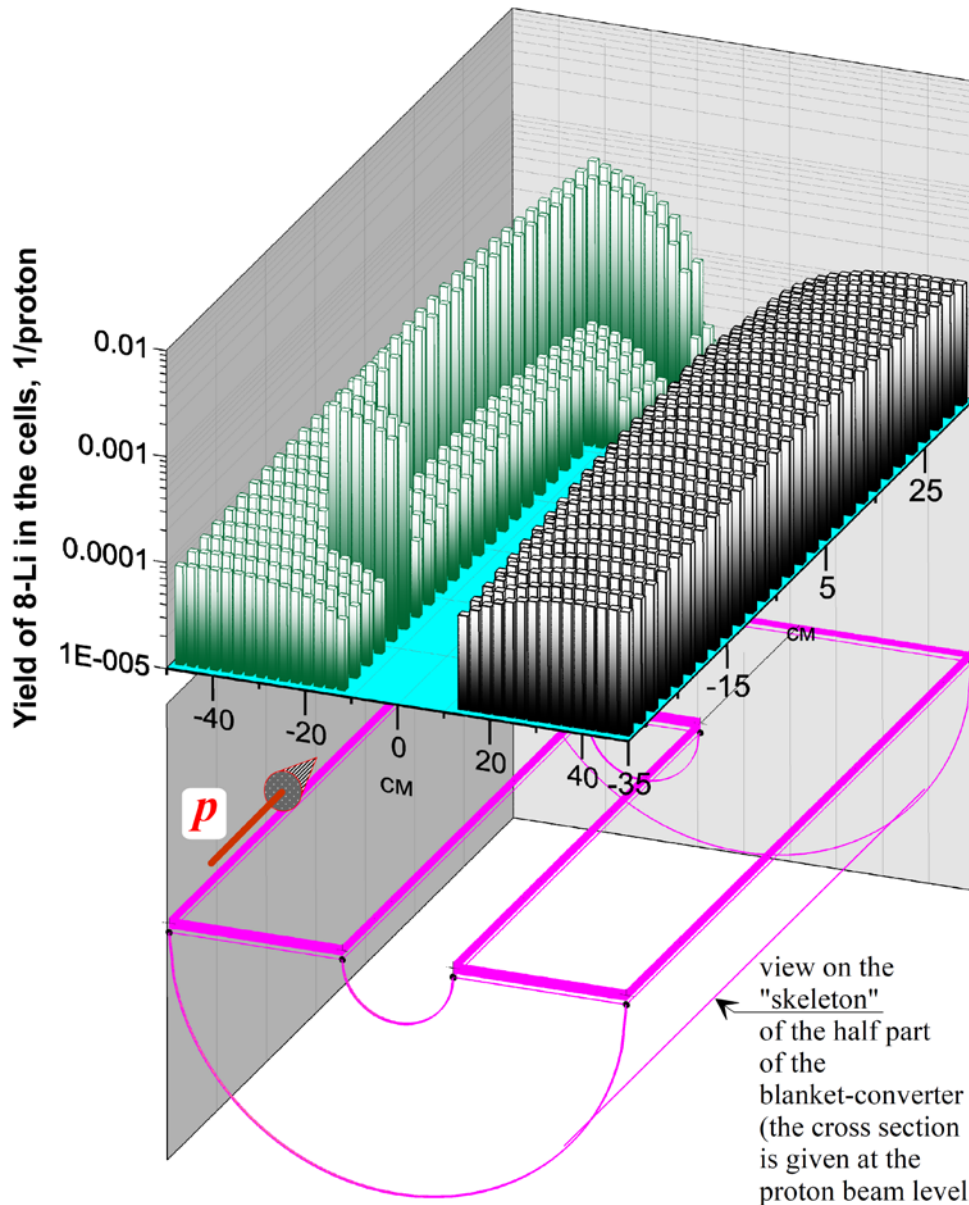


Fig. 4. Yield of  $^8\text{Li}$  in the cells of the lithium blanket for accelerator scheme at the proton energy 200 MeV. The data are normalized per proton of the beam. The dimensions of the blanket are indicated. The left part of the distribution (at the  $X < 0$ ) corresponds the yields in cells for discussed geometry of the blanket with the thin  $^7\text{Li}$  metal layer (see Fig. 3b), in which the strong increase of  $^8\text{Li}$  yield (compare the cells filled with  $^7\text{LiOD}$  heavy water solution) is obtained. For comparison (of the strong effect from the lithium metal) the right part (at the  $X > 0$ ) shows the  $^8\text{Li}$  yield in the cells in case of the blanket (with the same dimensions) filled with  $^7\text{LiOD}$  heavy water solution (i.e., without the lithium metal layer).

In the works [25,26] the authors proposed to construct the lithium  $\bar{\nu}_e$ -source (with the similar to [27] geometry and the same purity of  $^7\text{Li}$ ): the scheme was based on the proton accelerator ( $E_p = 60$  MeV) and neutron generating  $^9\text{Be}$ -target in the cylindrical lithium blanket-converter (with height 150 cm and diameter 200 cm) filled with metallic lithium. The

expected  $N_{\bar{\nu}}$ -flux from the converter [25,26] during 5 years (for 90% using of time and accelerator current  $I=10$  mA) is evaluated as  $1.29 \cdot 10^{23}$ . For comparison the considered here compact  $\bar{\nu}_e$ -source (length  $L=70$  cm, diameter 99 cm; Fig. 4) with:  $^{174}\text{W}$ -target, 200-MeV proton beam of the current in order smaller – 1 mA, a data-taking period of 5 yr and the same useful time of 90% will ensure the total  $\bar{\nu}_e$ -flux as  $1.00 \times 10^{23}$ . The requested highly enriched  $^7\text{Li}$  mass can be decrease in 90 times: from 6.1 t (in [25,26] case) down to 67.5 kg.

### 3. Conclusion

It was considered two principal variants of intensive  $\bar{\nu}_e$ -source with hard spectrum ( $E_{\bar{\nu}}^{\text{max}} \approx 13$  MeV and average energy 6.5 MeV) produced by  $^8\text{Li}$  at (n, $\gamma$ )-activation of  $^7\text{Li}$  isotope (with purity 99.99%): on the base of proton accelerator and neutron generating tungsten target.

The construction of the  $\bar{\nu}_e$ -source in tandem scheme of accelerator plus neutron producing target allows to work in the pure  $^8\text{Li}$ -spectrum excluding the large spectrum errors arisen in case of the reactor neutrino source. The evident advantage of the accelerator variant is the possibility to ensure the strong decrease of the requested high purified  $^7\text{Li}$  mass. The optimized scheme gives the possibility to minimize the mass of  $^7\text{Li}$  (purification 99.99%) down to 67.5 kg. Realization of the accelerator variant allows to create the very compact  $\bar{\nu}_e$ -source with dimension reduced to 70 cm that is exclusively important for checking of short length of oscillation in sterile neutrino experiments.

The author sincerely thanks Yu.S. Lutostansky and M.D. Skorokhvatov for interest and helpful discussion.

### REFERENCES

1. F. Reines F. and C.L. Cowan Jr., Phys. Rev. **92**, 830 (1953).
2. P. Huber, Phys. Rev. C **84**, 024617 (2011).
3. A.C. Hayes, J.L. Friar, G.T. Garvey, Gerard Jungman, and G. Jonkmans, Phys. Rev. Lett. **112**, 202501 (2014).
4. V.A. Korovkin, S.A. Kodanov, A.D. Yarichin, A. A. Borovoi, V.I. Kopeikin, L.A. Mikaelyan, V.D. Sidorenko, Soviet Atomic Energy **56**, 233 (1984).
5. V. I. Kopeikin, Phys. At. Nucl. **75**, 143 (2012).
6. A.C. Hayes, J.L. Friar, G.T. Garvey, D. Ibeling, G. Jungman, T. Kawano, R.W. Mills, Phys. Rev. D **92**, 033015 (2015).
7. V.G. Aleksankin, S.V. Rodichev, P.M. Rubtsov, P.A. Ruzansky. and F.E. Chukreev. *Beta and antineutrino radiation from radioactive nuclei* (Energoatomizdat, Moscow, 1989), ISBN 5-283-03727-4 (in Russian).
8. A.J. Koning, D. Rochman, J. Sublet, N. Dzysiuk, M. Fleming, S. van der Marck, Nucl. Data Sheets **155**, 1 (2019).
9. Zhigang Ge, Ruirui Xu, Haicheng Wu, Yue Zhang, Guochang Chen, Yongli Jin, Nengchuan Shu, Yongjing Chen, Xi Tao, Yuan Tian, Ping Liu, Jing Qian, Jimin Wang, Huanyu Zhang, Lile Liu, and Xiaolong Huang, EPJ Web of Conferences **239**, 09001 (2020).

10. Yu.S. Lyutostansky and V.I. Lyashuk, Reactor neutrons-antineutrino converter on the basis of lithium compounds and their solutions, *Sov. Atom. Energ.* **69**, 696 (1990).
11. Yu.S. Lyutostansky and V.I. Lyashuk, *Nucl. Sci. Eng.* **117**, 77 (1994).
12. Yu.S. Lutostansky, V.I. Lyashuk, *Physics of Elementary Particles and Atomic Nucl., Lett.* **2**, 60 (2005).
13. V.I. Lyashuk, Yu.S. Lutostansky, arXiv:1503.01280v2 [physics.ins-det].
14. V.I. Lyashuk, Yu.S. Lutostansky, *Bull. Russ. Acad. Sci. Phys.* **79**, 431 (2015).
15. T. Adam, F. An, G. An, Q. An, N. Anfimov, V. Antonelli, G. Baccolo, M. Baldoncini, E. Baussan, M. Bellato, L. Bezrukov, D. Bick, S. Blyth, S. Boarin, A. Brigatti, T. Brugiere, et al. (JUNO Collaboration), arXiv:1508.07166v2 [physics.ins-det].
16. V.I. Lyashuk and Yu. S. Lutostansky, *Jetp Lett.* **103**, 293 (2016).
17. V.I. Lyashuk, V.I., *Results in Phys.* **6**, 961 (2016).
18. V.I. Lyashuk, *Particles and Nuclei, Letters* **14**, 456 (2017).
19. V.I. Lyashuk, arXiv: 1609.02127 [physics.ins-det].
20. M. Maltoni, T. Schwetz, *Phys. Rev. D* **76**, 093005 (2007).
21. J. Kopp, M. Maltoni, T. Schwetz, *Phys. Rev. Lett.* **107**, 091801 (2011).
22. J.M. Conrad, C.M. Ignarra, G. Karagiorgi, M.H. Shaevitz, and J. Spitz, *Advances in High Energy Physics* **2013**, Article ID 163897, (2013).
23. M. Dentler, Á. Hernández-Cabezudo, J. Kopp, P. Machado, M. Maltoni, I. Martinez-Soler and T. Schwet, *J. High Energ. Phys.* **2018**, 10 (2018).
24. V.V. Khrushov, S.V. Fomichev, and S.V. Semenov, *Phys. Atom. Nuclei* **84**, 328 (2021).
25. A. Bungau, A. Adelman, J.R. Alonso, W. Barletta, R. Barlow, L. Bartoszek, L. Calabretta, A. Calanna, D. Campo, J.M. Conrad, Z. Djurcic, Y. Kamyshkov, M.H. Shaevitz, I. Shimizu, T. Smidt, et. al., *Phys. Rev. Lett.* **109**, 141802 (2012).
26. A. Bungau, R. Barlow, M. Shaevitz, J. Conrad, J. Spitz, arXiv:1205.5790v1 [physics.acc-ph].
27. Yu.S. Lutostansky and V.I. Lyashuk, *The concept of a powerful antineutrino source*, *Bull. Russ. Acad. Sci. Phys.* **75**, 468 (2011).